

## Photoresponsive porous organosilicas\*

Hermenegildo García<sup>‡</sup>

*Instituto de Tecnología Química, Universidad Politécnica de Valencia, Avda. de los Naranjos, 46022-Valencia, Spain*

*Abstract:* Novel structured functional hybrid materials can be obtained by incorporating photoresponsive organic components into the silicate walls of periodic mesoporous silicates. Two such materials are described, containing either viologens or stilbene analogs. Thermal or photochemical activation of viologen units generates the corresponding radical cations, whose lifetime can vary from months to milliseconds, depending on the surfactant content of the solid. In a second example, the porosity and tortuosity of the silicate can be modulated by irradiation of an organosilica containing a stilbene-like moiety.

### INTRODUCTION

The synthesis of mesoporous materials [1] by Mobil researchers in 1991 constituted a significant breakthrough in the field of host–guest chemistry [2] and catalysis [3]. Ordered mesoporous silicas overcame the limitation of microporous zeolites in terms of the molecular size of the organic molecules that can be incorporated within the porous silicate structure. MCM silicates exhibit a monodal pore size distribution that can be controlled during the synthesis from 2 to 10 nm, thus resulting in a logical extension of the zeolite supramolecular chemistry, limited to the micropore domain (pore size 0.5–1.4 nm) [2]. The most common and easy-to-prepare structured mesoporous material is MCM-41; its internal voids are formed by an array of parallel hexagonal channels typically of 3–4 nm diameter. They have a specific surface area above  $700 \text{ m}^2 \times \text{g}^{-1}$  and a pore volume of about  $0.8 \text{ mL} \times \text{g}^{-1}$ . The remarkable pore size and internal volume places MCM-41 materials in the top echelon of porous materials, being particularly well suited to adsorb large organic guests in their interior. Many systems have been reported in which the molecular properties of the guest are varied upon adsorption into MCM-41 particles [2]. However, owing to the unidirectional topology of the MCM-41 voids and their uniform pore size, adsorbates could, in principle, also be desorbed and extracted out of the mesopores. To avoid desorption of the guest, methodologies have been developed to link the adsorbate covalently through a tether to the silicate walls of appropriately modified MCM-41.

More recently, a new type of mesoporous material has been reported in which the organic component is introduced during the synthesis of the silicate and forms part of the wall of the mesoporous silicate. This can be achieved using organic substrates functionalized with two terminal trialkoxysilyl groups. This organosilicon compound is added to the synthesis gel in the desired proportion together with an inorganic source of silicon atoms, typically tetraethoxyorthosilicate (TEOS). The crystallization of the hybrid organic/inorganic material is performed under conventional MCM-41 conditions (80 °C, cetyltrimethylammonium bromide, CTABr, as surfactant, basic medium, several days) using a gel containing organic compounds bound to silicon atoms. As the hydrolysis and condensation of the polyalkoxysilane precursors progress and the silicate particle develops, the solid contains a certain amount of organic substructure within the walls [4–6]. The term periodic mesoporous organosilica

\*Lecture presented at the XIX<sup>th</sup> IUPAC Symposium on Photochemistry, Budapest, Hungary, 14–19 July 2002. Other presentations are published in this issue, pp. 999–1090.

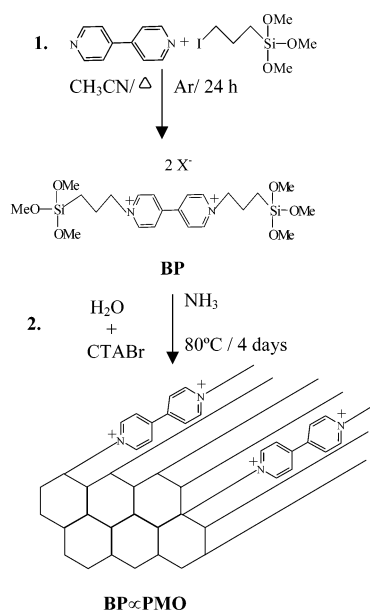
<sup>‡</sup>E-mail: hgarcia@qim.upv.es

(PMO) has been coined for this type of organic/inorganic hybrid solid. These structured PMO materials can serve to prepare functional materials, in which the organic component would impart some desirable physical, chemical, or photochemical property to the solid, while the inorganic silica framework continues to provide the mesoporous periodic ordering and robustness of the material. The work presented here exploits the methodology of PMO preparation to obtain photoresponsive materials.

## RESULTS AND DISCUSSION

We will comment on two related examples to illustrate the opportunities that these materials offer. The first PMO solid contains viologen units forming part of the silicate wall. Viologens have been widely used to form charge-transfer complexes with electron-rich molecules and also as electron acceptors in photoinduced electron transfer [2]. The corresponding radical cation, generated upon electron transfer, can be characterized unambiguously by Raman and optical spectroscopy. Because of their blue/green color, viologen radical cations also find application in electro- and photochromic devices. The photochemistry of viologens has been studied in numerous heterogeneous systems, including microporous zeolites and mesoporous MCM-41 aluminosilicates [7], materials closely related to PMOs. Thus, we undertook the synthesis of PMOs containing viologen units covalently bound to the walls ( $\text{BP}\infty\text{PMO}$ ) to determine the properties of these novel viologen-containing PMOs, particularly comparing their behavior with that of a related system in which an analogous viologen is merely adsorbed on mesoporous MCM-41.

The synthesis of  $\text{BP}\infty\text{PMO}$  was accomplished from *N,N'*-bis(triethoxysilylpropyl)-4,4'-bipyridinium (BPSi) diiodide by condensing this silicon compound with TEOS in the presence of CTABr under the usual conditions employed for MCM-41 (Scheme 1). A series of  $\text{BP}\infty\text{PMO}$  solids were prepared in which the TEOS/BPSi molar ratio in the mother gel was systematically varied from 95:5 to 50:50.



**Scheme 1** Procedure for the preparation of viologen-containing  $\text{BP}\infty\text{PMO}$  solids.

The formation of well-crystallized solids was assessed by powder X-ray diffraction (XRD), which showed the characteristic pattern of MCM-41, although the structural ordering of the solid decreases as

the BPSi content increases. Upon removal of the CTABr by solid–liquid extraction, the characteristic XRD pattern remains for most PMOs with only minor decrease in the peak intensity as compared to the as-synthesized BP $\infty$ PMO in which the pores are completely full of CTABr. Figure 1 shows selected XRD patterns.

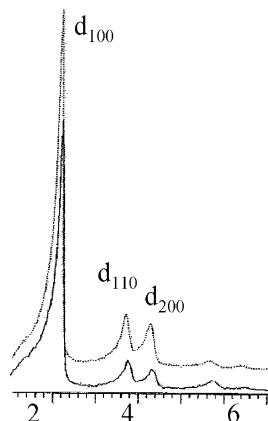


**Fig. 1** Powder XRD spectrum of as-synthesized BP $\infty$ PMO (upper diffractogram) and after removal of the CTABr surfactant by acid extraction in organic solvents (lower diffractogram). The characteristic MCM-41-like peaks are identified. It is remarkable that the structure remains after CTABr removal.

The presence of BP in the solid can be demonstrated by spectroscopy. In the diffuse-reflectance UV–vis spectrum of BP $\infty$ PMO, an intense band at 280 nm can be recorded. In the Fourier transform infrared (FT-IR), the most characteristic absorption band of BP appears at 1630  $\text{cm}^{-1}$ , which corresponds to the stretching vibration of the  $-\text{C}=\text{N}^+$  bond of the heterocyclic rings. Importantly, the spectra remain unchanged upon complete removal of CTABr (Fig. 2). This failure to extract BP in comparison to CTABr constitutes the strongest (although indirect) evidence supporting the covalent binding of BP on the silicate walls.  $^{29}\text{Si}$  NMR of the BP $\infty$ PMO also reveals the presence of a distinct peak at  $-70$  ppm, corresponding to  $(\text{O})_3\text{Si}-\text{CH}_2-$  present on BP having at least two other Si atoms in the next coordination sphere. However, the limited resolution of solid-state NMR precludes an assignment of the number of individual signals.

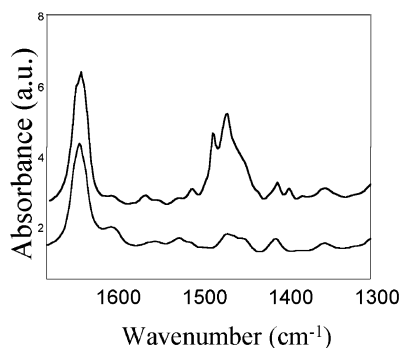


**Fig. 2** FT-IR spectra of as-synthesized BP $\infty$ PMO (TEOS:BP 0.85:0.15) recorded at room temperature (upper spectrum) and after degassing at 200  $^{\circ}\text{C}$  for 1 h at  $10^{-2}$  Pa. (lower spectrum). The decrease in the intensity of the 1470  $\text{cm}^{-1}$  band corresponds to the desorption of the structure-directing agent.

The formation of CT complexes between BP and halides is responsible for the broad, featureless bands in the diffuse-reflectance UV–vis spectrum of BP $\infty$ PMO. This band increases in intensity with the BP content of the solid, but also when the diiodide BPSi precursor is converted into dibromide prior to synthesis of the solid. The improved resolution derives from the collapse of the two broad CT bands {[BP-I] and [BP-Br] complexes} into a single one (Fig. 3).

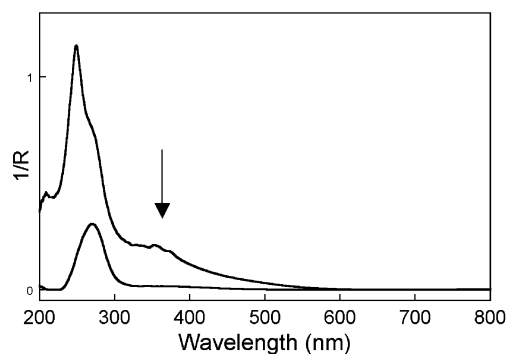


**Fig. 3** Diffuse-reflectance spectra of as-synthesized BP $\infty$ PMO (upper plot) and after removal of the CTABr surfactant (lower plot). The arrow indicates the characteristic CT band due to the viologen-Br complex.

Upon irradiation of BP $\infty$ PMO in a sealed quartz cell, the exposed surface becomes blue and the diffuse-reflectance UV–vis spectrum of the surface reveals the formation of the corresponding viologen radical cation. The color intensity grows with the irradiation time. After prolonged irradiation, the percentage of BP converted into BP $^{\bullet+}$  can be estimated based on the relative intensity of the UV–vis spectral bands corresponding to the radical cation (600 nm) and that of the precursor (280 nm) corrected by the relative extinction coefficients. Thus, more than 90 % of the BP present in the exposed surface of the solid probed in the diffuse-reflectance UV–vis spectroscopy has been transformed into BP $^{\bullet+}$ . Furthermore, the blue color persists in the sealed cell for longer than one month. In contrast, if the mesopores of the material are devoid of CTABr, and therefore, accessible to other reagents such as oxygen and moisture, lamp irradiation does not produce any visual effect. However, fast spectroscopic techniques combined with laser flash photolysis reveals again that BP $^{\bullet+}$  is also formed in the BP $\infty$ PMO solid devoid of CTABr, although as a transient decaying in the millisecond time scale (Fig. 4).

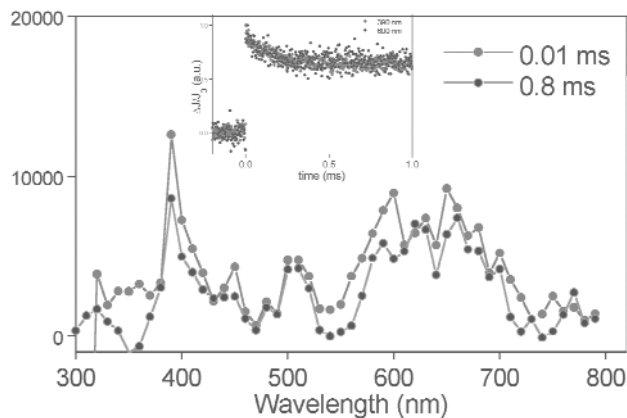
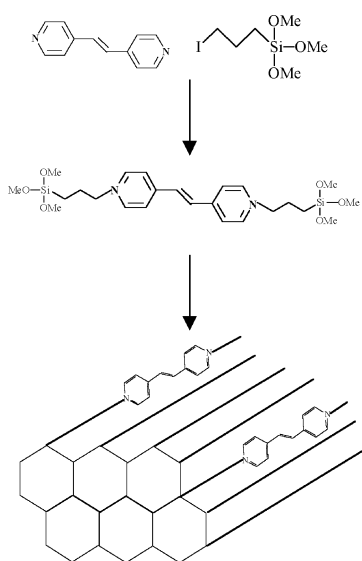


**Fig. 4** Transient diffuse-reflectance UV–vis spectra recorded 0.01 or 0.8 ms after 266-nm laser excitation of BP $\infty$ PMO. The inset shows the coincident decay of the signals recorded at 390 and 600 nm.

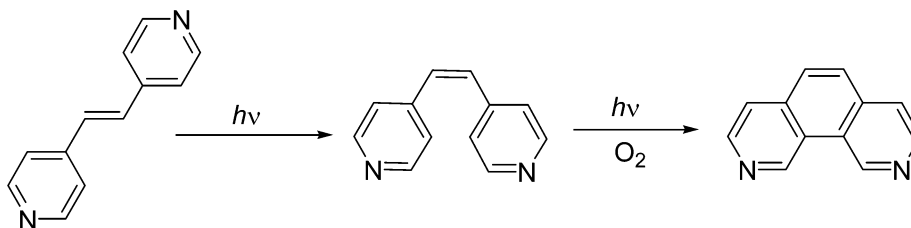
According to these data, it should be possible, in principle, to tune the photochromic effect observed for BP $\infty$ PMO from milliseconds to months by simple control of the amount of CTABr filling the pores.

A second example of the opportunity to design photoresponsive PMO materials consists in the synthesis of a structured, mesoporous silicate containing bis(pyridyl)ethylene in the walls *t*-BE $\infty$ PMO. The synthesis is achieved from the corresponding *N,N'*-bis(triethoxysilylpropyl) derivative following a procedure analogous to that used for the preparation of BP $\infty$ PMO (Scheme 2). This *t*-BE $\infty$ PMO solid was characterized by powder XRD, diffuse-reflectance UV–vis, and IR spectroscopies. The structure of the solid is maintained after extraction of the CTABr. All available data are consistent with those reported for PMOs and indicate that the bipyridinium ethylene units are covalently anchored to the mesoporous structure of MCM-41.



**Scheme 2** Synthetic scheme for the preparation of *t*-BE $\infty$ PMO.

According to the well-known photochemical behavior of stilbenes and related compounds, irradiation of *t*-1,2-bis(4-pyridyl)ethylene in aerated acetonitrile solutions leads to a photoinduced *trans*–*cis*-isomerization; subsequently, the *cis*-isomer undergoes photocyclization to a diazaphenanthrene, Scheme 3. The leading idea behind the preparation of *t*-BE $\infty$ PMO was to synthesize a photoactive silicate in which the *t*-BE occupying framework positions would undergo this photochemical *trans*–*cis*-isomerization; such a transformation was expected to lead to a measurable change in the porosity of the solid.



**Scheme 3** Photochemistry of *t*-BE.

To demonstrate this effect, one *t*-BE $\infty$ PMO sample (TEOS:*t*-BE 98.5:1.5) devoid of CTABr was submitted to lamp irradiation. An identical sample was simultaneously submitted to the same manipulation, except that it was protected from light. After irradiation, the pore size distribution of the two twin samples was determined by the standard isothermal nitrogen adsorption. These measurements (Fig. 5) prove that the material has altered its pore size as response to the irradiation, thus, reflecting shape variations due to differences in the *cis/trans* configuration of the C=C bonds of the organic component. Porous solids whose pore diameter can be varied upon light excitation will have application in photoresponsive membranes, in which the diffusion of a mixture through the pores could be influenced by irradiation.

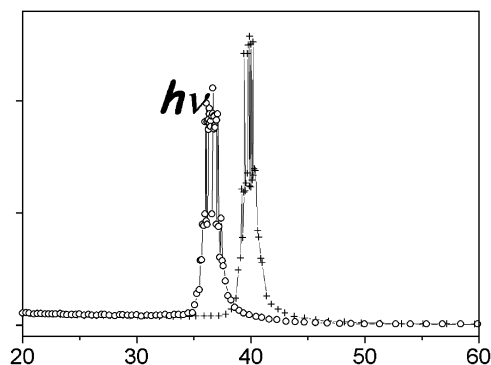


**Fig. 5** Pore size distribution of a *t*-BE $\infty$ PMO sample devoid of CTABr before (unlabeled) and after UV irradiation (labeled as *hν*).

In conclusion, the above examples serve to illustrate the new opportunities that novel periodic mesoporous organosilicas offer for the development of *smart or advanced functional materials*. Most of the fundamentals that are going to be applied derive from the basic knowledge gained in host–guest photochemistry, particularly, intrazeolite photochemistry obtained since the 1980s. Because of the significant progress achieved in the *shaping* of these powders into oriented films and membranes of regular particle size, these materials are now closer to application as components in devices.

## ACKNOWLEDGMENTS

Financial support by the Spanish DGES (Grant MAT2000-1767-CO2-01) is gratefully acknowledged. The author thanks Drs. M. Alvaro and B. Ferrer for their collaboration in the synthesis of PMOs.

## REFERENCES

1. C. T. Kresge, M. E. Leonowicz, W. J. Roth, J. C. Vartuli, J. S. Beck. *Nature* **359**, 710–712 (1992).
2. H. Garcia and H. D. Roth. *Chem. Rev.* **102**, 3947–4008 (2002).
3. A. Corma. *Chem. Rev.* **97**, 2373–2419 (1997).
4. C. Yoshina-Ishii, T. Asefa, N. Coombs, M. J. MacLachlan, G. A. Ozin. *Chem. Commun.* 2539–2540 (1999).
5. M. J. MacLachlan, T. Asefa, G. A. Ozin. *Chem. Eur. J.* **6**, 2507–2511 (2000).
6. S. Inagi, S. Guan, Y. Fukushima, T. Oshuna, O. Terasaki. *J. Am. Chem. Soc.* **121**, 9611–9614 (1999).
7. M. Alvaro, H. García, S. García, F. Marquez, J. C. Scaiano. *J. Phys. Chem.* **101**, 3043–3051 (1997).